



Application of fuzzy systems on the numerical solution of the elliptic PDE-constrained optimal control problems

Masoomeh Azizi¹, Majid Amirfakhrian^{1,2,*}, and Mohammad Ali Fariborzi Araghi¹

¹Department of Mathematics, Central Tehran Branch, Islamic Azad University, Tehran, Iran.

²Department of Computer Sciences, University of Calgary, Calgary, Canada.

Abstract

This paper presents a numerical fuzzy indirect method based on the fuzzy basis functions technique to solve an optimal control problem governed by Poisson's differential equation. The considered problem may or may not be accompanied by a control box constraint. The first-order necessary optimality conditions have been derived, which may contain a variational inequality in function space. In the presented method, the obtained optimality conditions have been discretized using fuzzy basis functions and a system of equations introduced as the discretized optimality conditions. The derived system mostly contains some nonsmooth equations and conventional system solvers fail to solve them. A fuzzy-system-based semi-smooth Newton method has also been introduced to deal with the obtained system. Solving optimality systems by the presented method gets us unknown fuzzy quantities on the state and control fuzzy expansions. Finally, some test problems have been studied to demonstrate the efficiency and accuracy of the presented fuzzy numerical technique.

Keywords. Optimal control problems, Fuzzy system, Fuzzy basis functions, Universal approximation properties, Poisson's equation, Optimality conditions, Semi-smooth Newton method.

2010 Mathematics Subject Classification. 49M15, 90C70, 35J05, 49K20.

1. INTRODUCTION

When Lotfi A. Zadeh introduced fuzzy logic six decades ago, no-one imagined that it would be so effective in today's human life. Fuzzy logic and related innovations have deeply affected almost all features of our life from smart instruments such as washing machines, elevators, cars, etc. to social network communications and network search engines. The simplicity and interpretability property of fuzzy logic systems in "compute with words", makes it possible to model complex phenomena with fuzzy roles close to natural language.

Optimal control theory similar to other scientific areas has been greatly influenced by the rapid development of fuzzy logic theory and its applications. The flexibility and convenience of fuzzy logic in the explanation of the uncertainty properties of phenomena has made new opportunities in the control system design. Furthermore, the descriptive nature of fuzzy logic and its capability to study incomplete, subjective and inconsistent information provide many usable and advantageous methods in optimal control researches [1].

Providing the novel, efficient and flexible methods to estimate control and state functions is one of the various applications of fuzzy logic systems in this field [22]. Based on this approximation method, various numerical algorithms for the optimal control problem (OCP) have been designed. The success of these numerical approaches depends on the ability of fuzzy systems in function approximation [30].

OCPs can be found in almost all branches of sciences with various kinds of objective functionals and differential constraints in diverse forms. The most common form is optimal control of ordinary differential equations [21]. Whereas,

Received: 24 April 2020 ; Accepted: 24 April 2021.

* Corresponding author. Email: amirfakhrian@iauctb.ac.ir, majid.amirfakhrian@ucalgary.ca.

in the real world, many phenomena have been modelled by partial differential equations (PDEs). Therefore, the optimal control of PDEs has become an important practical problem since the past decade. For instance, heat conduction, freezing processes, diffusion, fluid flows and electromagnetic waves can be formulated by PDEs and optimal control of them has been subjected to much scientific research in the recent years [27].

In this paper, we focus on the numerical solution of an OCP governed by an elliptic PDE. The considered problem is optimal control of the Poisson's equation, which is a practical problem in heat distribution field. The optimal state and control of this problem are almost non-smooth. Moreover, if the problem is governed by state or control box constraints, the optimality conditions involve with a variational inequality (VI). In these cases, the problem domain can be divided into two sub-domains where the constrained variable value reaches the bounds of permissible values in one of them but not in the other. Due to the priori unknown boundary between these two areas, such a problem can be categorized as "free boundary problems" [15] and solving it needs extra strategies to catch this free boundary.

Many numerical approaches to the considered problem have been studied so far. Traditionally, finite element methods were the first choice [2, 3, 13, 20]. For instance, Becker et al. developed a finite element method for elliptic PDE-constrained OCPs in [3]. They used the Lagrangian method to yield the necessary optimality conditions in the form of the indefinite boundary value problems and then used adaptive Galerkin finite element method to solve it. Later, to solve the considered problem, an adaptive finite element method based on the posteriori error estimates was presented in [19]. A smoothed-penalty algorithm for this problem has also been introduced in [12]. Moreover, active set strategy utilized for the same problem by Bergounioux et al. [4]. As a newer instrument of numerical analysis in non-square domains, radial base functions (RBFs) were also used to solve this kind of problems [25]. Pearson [23] demonstrated some RBF-based methods for this problem with no constraints imposed on the state and control functions. He developed straight and symmetric collocation methods in solving Poisson's equation to solve an OCP, either. Also, he presented an approximation of Schur's complement for preconditioners of the given problem in [24]. Moreover, the adaptive wavelet collocation method for the same class of distributed elliptic OCPs has been introduced in [15]. Ghasemi and Effati used the artificial neural network and tried to introduce a new computational method to solve this problem in [10]. Finally, it is worth to mention that the authors of this paper introduce a fuzzy-based active set strategy to solve the same problem in [1].

In this work, we develop a new numerical method based on the fuzzy systems to solve the distributed elliptic OCP. In the presented method, the first-order necessary optimality conditions of the problem are obtained. It is shown that these conditions are a coupled system of elliptic PDEs with Dirichlet boundary conditions that may or may not be associated with a variational inequality. Then we use universal approximation property of the fuzzy basis functions (FBFs) to discretize the control and state functions. Thereupon, the discretized problem is studied in two separate cases: First, whenever the state and control is not constrained and discretizing the optimality system leads to a finite-dimensional linear equations system. Second, whenever the state or control function is limited by box constraint in the problem. In this case, a semi-smooth Newton method is introduced to solve the discretized optimality conditions, namely "the finite-dimensional mixed variational inequality problem".

In fact, providing an algorithm based on fuzzy systems to approximate non-smooth solutions of the given problem is the main goal of this work. It is worth noting that in spite of the widespread applications of fuzzy logic in scientific topics, its implementation in numerical analysis has so far been limited to smooth problems [7]. But the considered FBFs in this paper have universal approximation properties on continuous function spaces. It means that the considered FBFs can approximate a non-smooth but continuous function to any arbitrary degree of accuracy. This fact is our main motivation for illustrating the capability of the fuzzy-system-based approaches to solve non-smooth problems such as the considered OCP.

The structure of this paper is outlined as follows:

In the next section, after establishing the formulation of considered model, we derive the first-order necessary optimality conditions of the considered OCP are discussed.

In section 3, a brief review of fuzzy systems and FBFs is mentioned.

The main section of this paper is section 4, where we introduce a fuzzy-system-based method to solve the considered problem.



Finally, section 5 is devoted to numerical examples to show the accuracy and validity of the presented fuzzy-based algorithm.

2. OPTIMAL CONTROL OF POISSON’S EQUATION

Let Ω is a spatial domain occupied by a body. The temperature of this body is affected by a heater/cooler source in Ω and is fixed on the boundary of the domain, which is denoted by $\partial\Omega$. Also, denote the distributed temperature and the distribution of the heater/cooler source as the state function y and the control function u , respectively. They can be related by the following Poisson’s equation with the Dirichlet boundary condition:

$$\begin{aligned} \Delta y &= -ku && \text{in } \Omega, \\ y &= 0 && \text{on } \partial\Omega. \end{aligned} \tag{2.1}$$

We aim to find the state function y_{opt} on the whole Ω as close as possible to a desired temperature pattern z . It must be done by the minimum amount of heat source consumption. The mentioned problem can be modelled as the minimizing problem of the objective functional [27]

$$J[u, y] := \frac{1}{2} \left(\int_{\Omega} |y - z|^2 dx + \gamma \int_{\Omega} |u|^2 dx \right) \tag{2.2}$$

constrained by the elliptic PDE (2.1). Here, γ is a positive regularization parameter between the two parts of the objective functional. In some cases, a technical restriction for the heater/cooler source power forces us to consider an additional box constraint on the control function such as

$$g(x) \leq u(x) \leq h(x) \quad x \in \Omega. \tag{2.3}$$

Thus, the aforesaid problem can be described as the following mathematical model [27]:

$$\text{Min } J[u, y] = \frac{1}{2} \left(\int_{\Omega} |y - z|^2 dx + \gamma \int_{\Omega} |u|^2 dx \right) \tag{2.4a}$$

$$\text{such that } (y, u) \in \mathcal{Y} \times \mathcal{U}, \tag{2.4b}$$

$$\Delta y(x) = -ku(x) \quad x \in \Omega, \tag{2.4c}$$

$$y(x) = 0 \quad x \in \partial\Omega. \tag{2.4d}$$

In the lack of any extra constraint on the control and state functions, the admissible functions sets can be considered as

$$\mathcal{Y} = H_0^1(\Omega) := \{v \in H^1(\Omega) \mid v|_{\partial\Omega} = 0\} \quad \text{and} \quad \mathcal{U} = L^2(\Omega).$$

Furthermore, when the control function is limited by the box constraint (2.3), the admissible control functions set must be changed to

$$\mathcal{U} = \{v \in L^2(\Omega) \mid g(x) \leq v(x) \leq h(x)\}. \tag{2.5}$$

Such choices for the admissible control and state functions are sensible owing to existence and uniqueness of the solutions, which is clarified below.

One can define the following continuous linear mapping as a control-to-state operator:

$$S : L^2(\Omega) \rightarrow H_0^1(\Omega) (\subset L^2(\Omega)), \quad u \mapsto y(u).$$

Therefore, the OCP (2.4) reduces to a non-constrained quadratic optimization problem in $\mathcal{U} \subseteq L^2(\Omega)$ in terms of the control function u as

$$\min_{u \in \mathcal{U}} \hat{J}[u] = \frac{1}{2} \left(\int_{\Omega} |S(u) - z|^2 dx + \gamma \int_{\Omega} |u|^2 dx \right). \tag{2.6}$$

The existence and uniqueness of the reduced problem solution are guaranteed by a well-known result about quadratic convex Hilbert optimization problem. It can be found in [27]. Furthermore, the relation between a VI problem and an optimization problem has been expressed in the following lemma:



Lemma 2.1 ([11]). *Assume that the functional $\mathcal{F} : K \rightarrow \mathbb{R}$ is a convex and Fréchet differentiable operator where K is a nonempty closed convex subset of a Hilbert space $\{H, \langle \cdot, \cdot \rangle\}$. Then $\bar{w} \in K$ is a solution to the minimization problem*

$$\min_{w \in K} \mathcal{F}[w],$$

if and only if \bar{w} satisfies the VI

$$\langle \mathcal{F}'[\bar{w}], v - \bar{w} \rangle \geq 0 \quad \forall v \in K. \tag{2.7}$$

Remark 2.2. If K is a subspace, then the VI (2.7) can be reduced to following equality:

$$f'[\bar{w}] = 0. \tag{2.8}$$

Now, one can derive the optimality conditions of the OCP (2.4) by computing the Fréchet differential of \hat{J} and applying Lemma 2.1 on the reduced problem (2.6). So, $u_{opt} \in \mathcal{U}$ is a minimizer for the OCP (2.4) if and only if

$$\langle S^*(S(u_{opt}) - z) + \gamma u_{opt}, u - u_{opt} \rangle \geq 0 \quad \forall u \in \mathcal{U}, \tag{2.9}$$

where S^* is the adjoint operator of S and it can be identified by the following lemma.

Lemma 2.3 ([27]). *The adjoint operator related to the Dirichlet Poisson's equation (2.1), denoted by $S^* : L^2(\Omega) \rightarrow L^2(\Omega)$, is given by*

$$S^*w = kv, \tag{2.10}$$

where $v \in H_0^1(\Omega)$ is the weak solution of

$$\begin{aligned} \Delta v &= -w \quad \text{in } \Omega, \\ v &= 0 \quad \text{on } \partial\Omega. \end{aligned}$$

By substituting $w = S(u_{opt}) - z$ in Eq. (2.10), we conclude $kv = S^*(S(u_{opt}) - z)$, where v satisfies the adjoint equations

$$\begin{aligned} kv &= S^*(S(u_{opt}) - z), \\ \Delta v &= z - S(u_{opt}) \quad \text{in } \Omega, \\ v &= 0 \quad \text{on } \partial\Omega. \end{aligned}$$

Thus, the optimality conditions can straightforwardly be summarized in the following theorem.

Theorem 2.4. *The functions $u \in \mathcal{U}$ and $y \in H_0^1(\Omega)$ are the optimal control and state functions of the OCP (2.4), respectively if and only if u, y and the related adjoint function $v \in H_0^1(\Omega)$ satisfy the following optimality system:*

$$\Delta y = -ku \quad \text{in } \Omega, \tag{2.11a}$$

$$\Delta v = z - y \quad \text{in } \Omega, \tag{2.11b}$$

$$\langle kv + \gamma u, w - u \rangle \geq 0 \quad \forall w \in \mathcal{U}, \tag{2.11c}$$

$$y = 0, v = 0, \quad \text{on } \partial\Omega. \tag{2.11d}$$

Remark 2.5. In the lack of the box constraint (2.4d), i.e., $\mathcal{U} = L^2(\Omega)$, it is easy to see that the VI (2.11c) reduces to the more simple equality

$$kv + \gamma u = 0. \tag{2.12}$$

In this case, we can eliminate the adjoint function by replacing $v = -\frac{\gamma}{k}u$ and the optimality system (2.11) can be simplified as

$$\Delta y = -ku \quad \text{in } \Omega, \tag{2.13a}$$

$$\gamma \Delta u = k(y - z) \quad \text{in } \Omega, \tag{2.13b}$$

$$u = 0 \quad \text{and} \quad y = 0 \quad \text{on } \partial\Omega. \tag{2.13c}$$



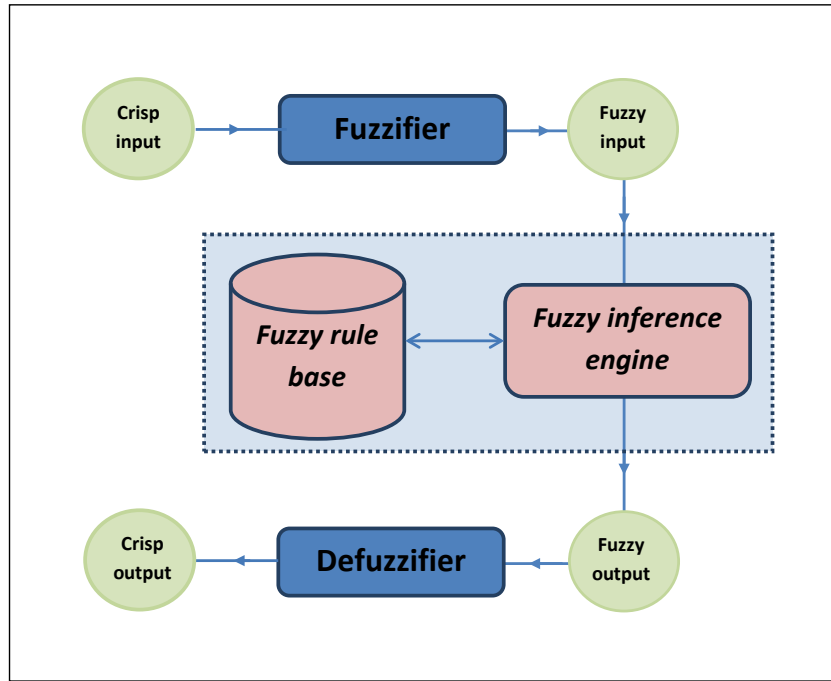


FIGURE 1. Fuzzy logic systems in an overview.

3. FUZZY SYSTEMS BACKGROUND

This section is devoted to a brief overview of the main concepts of a fuzzy logic systems whose overall configuration and relations is depicted in Figure 1. As can be seen, a fuzzy logic system consists of four main building blocks: a fuzzifier, a defuzzifier, an inference engine, and a fuzzy rule base.

The fuzzifier is a mapping from the crisp input points into the fuzzy sets in the input space $U \subset \mathbb{R}$, where a fuzzy set is characterized by a membership function $\mu : U \rightarrow [0, 1]$. Conversely, the defuzzifier performs a mapping from the fuzzy sets to the crisp points in the output space. Also, a fuzzy rule base is a collection of some linguistic statements in the form of "If (conditions), then (consequences)" as fuzzy rules that perform the fuzzy system. Finally, the fuzzy inference engine is the decision making logic, which is a simulation of human decision making procedure in order to determine a mapping by employing the fuzzy logic operations on the fuzzy rule base.

Each of the above can be assigned several values and make different types of fuzzy logic systems. In this paper, to avoid unnecessary complexities, we shall be concentrated on special and famous choices, i.e., a combination of singleton fuzzifier, height method defuzzifier, product inference and Gaussian membership functions to perform a fuzzy logic system.

Let K be a compact set and consider a multi-input-single-output fuzzy inference system $K \subset \mathbb{R}^n \rightarrow \mathbb{R}$. The singleton fuzzifier is one of the most commonly used fuzzifiers, which maps any $x \in K$ into a fuzzy set B in K with $\mu_B(x) = 1$ and $\mu_B(y) = 0$ for all $y \neq x$. Consider the following M fuzzy logic rules as the fuzzy rule base:

$$S^j : \quad \text{IF} \quad x_1 \text{ is } I_1^j \text{ and } x_2 \text{ is } I_2^j \text{ and } \dots \text{ and } x_n \text{ is } I_n^j, \\ \text{THEN} \quad y \text{ is } O^j, \quad j = 1, 2, \dots, M,$$

where y and x_i for $i = 1, 2, \dots, n$ are the output variable and the input variables, respectively. Moreover, I_i^j and O^j are linguistic statements characterized by fuzzy membership functions $\mu_{I_i^j}(x_i)$ and $\mu_{O^j}(y)$, respectively. Here, $\mu_{I_i^j}(x_i)$



is the Gaussian membership function given by

$$\mu_{I_i^j}(x_i) = a_i^j \exp \left[-0.5 \left(\frac{x_i - m_i^j}{\sigma_i^j} \right)^2 \right], \tag{3.1}$$

where $0 < a_i^j \leq 1$, and m_i^j and σ_i^j are real-valued parameters. Each S^j is a fuzzy implication $I_1^j \times \dots \times I_n^j \rightarrow O^j$, which is a fuzzy set in $U \times \mathbb{R}$ as $\mu_{I_1^j} \star \dots \star \mu_{I_n^j} \star \mu_{O^j}$. The most commonly used operation for \star is “product”. Moreover, the most commonly used method for the defuzzifier is the height method, which performs a mapping from the described fuzzy set into \mathbb{R} by the rule

$$y = f(\mathbf{x}) = \frac{\sum_{j=1}^M \bar{y}_j (\prod_{i=1}^n \mu_{I_i^j}(x_i))}{\sum_{j=1}^M (\prod_{i=1}^n \mu_{I_i^j}(x_i))}, \tag{3.2}$$

where \bar{y}_j belongs to the point in the output space Y and $\mu_{O^j}(\bar{y}) = 1$ is maximum.

Now, the following definition helps us to describe the Fuzzy system (3.2) more easily.

Definition 3.1. [30] Define a fuzzy basis function (FBF) by

$$\varphi_j(\mathbf{x}) := \frac{\prod_{i=1}^n \mu_{A_i^j}(x_i)}{\sum_{j=1}^M (\prod_{i=1}^n \mu_{A_i^j}(x_i))} \quad j = 1, 2, \dots, M. \tag{3.3}$$

It can be easily observed that the fuzzy system (3.2) can be expressed as

$$f(\mathbf{x}) = \sum_{j=1}^M \hat{f}_j \varphi_j(\mathbf{x}), \tag{3.4}$$

where $\hat{f}_j \in \mathbb{R}$ are all real-valued parameters as the singleton rule consequences.

Broadly speaking, it is not necessary to set all the parameters of FBFs in advance. However, these parameters can be optimized along with the \hat{f}_j 's by a back-propagation procedure [29]. It is worthwhile to mention that despite of the fact that FBFs are all nonlinear, setting all the parameters in the definition of φ_j at the inception of the FBFs expansion, \hat{f}_j 's will become the solely-free design parameters in the aforesaid fuzzy system [17]. Thus, the output f in Eq. (3.4) is clearly a linear combination of the remained design parameters.

Theorem 3.2. Suppose that f is a continuous real function defined on the compact set $C \subset \mathbb{R}^n$. For any arbitrary $\epsilon > 0$, there exists a fuzzy logic system f_ϵ in term of (3.2) such that

$$\sup_{x \in C} |f_\epsilon(x) - f(x)| \leq \epsilon. \tag{3.5}$$

Theorem 3.2 describes that the FBF expansion (3.4) has “universal approximation” property. It means that all continuous functions defined on a compact set can be uniformly approximated by a fuzzy logic system with any arbitrary degree of accuracy. The proof of this theorem is based on the well-known Stone-Weirstrass theorem in mathematical analysis and has been given by Wang in [30].

4. FBF-BASED ALGORITHM TO SOLVE AN OCP

In this section, we apply FBFs described in the previous section to propose a fuzzy-based novel numerical algorithm to solve the optimal control of the Poisson’s equation.

We consider two different modes for the OCP (2.4). The first mode is stated in the absence of Constraint (2.3), which leads to $\mathcal{U} = L^2(\Omega)$. In this case, the optimality system is a linear coupled elliptic PDE as (2.13). In the second mode, the control function is constrained with (2.3). Optimality system affected by this constraint and the VI (2.11c) isn’t imposed by it. Therefore, the presented numerical method must be combined with an effective VI solver. As it was mentioned before, non-smoothness on the optimal control and state is the main feature of the given problem. Such non-smoothnesses usually happen in an OCP if the optimality conditions contain the VIs. Thus, to obtain a



numerical solution for the given problem, we introduce a combination of a VI solver algorithm and a fuzzy logic system as a novel efficient algorithm.

In what follows, we describe the application of FBFs in the design of numerical algorithms for aforementioned two modes separately.

4.1. OCP Without any Box Constraint on Control. As stated above, an optimality system is a linear coupled elliptic PDE (2.13), which can be solved by FBFs. Let $I = \{1, 2, \dots, N\}$. Then I is a set of indices associated with the computational points Σ in $\Omega \subset \mathbb{R}^2$, i.e.,

$$\Sigma := \{\mathbf{x}^i = (x_1^i, x_2^i), \quad i \in I\}.$$

The set Σ can be partitioned into a set of the interior indices I_{int} and a set of the boundary indices I_{bd} , which are associated with computational point subsets $\partial\Sigma = \Sigma \cap \partial\Omega$ and $\Sigma_{int} = \Sigma \setminus \partial\Sigma$, respectively. They must be nonempty subsets.

By applying the function approximator described by Eq. (3.4), one can represent the state and control functions in terms of a fuzzy discretized form. Also, the approximation of derivatives of the given functions can be computed by direct differentiation on the FBFs, e.g.,

$$\Delta y(\mathbf{x}) = \sum_{j=1}^M \hat{y}_j(\Delta\varphi_j(\mathbf{x})). \tag{4.1}$$

Here, the main goal is to adjust the unknown parameters \hat{y}_j and \hat{u}_j as the fuzzy outputs of the functions expansions. It can be changed to the crisp outputs by exerting of defuzzifier formula given by Eq. (3.2). To this end, we can solve the linear equations obtained by employing the expansion given by Eq. (3.4) into Eq. (2.13) and collocating the obtained system in the points of Σ . From now on, in order to have a unique solution for the obtained system, we set $N = M$. It guarantees that the number of the unknown parameters should be as equal as to the equations in the discretized system. So, we can write

$$\left\{ \begin{array}{ll} \sum_{j=1}^M \hat{y}_j(\Delta\varphi_j(\mathbf{x}^i)) = -k \sum_{j=1}^M \hat{u}_j\varphi_j(\mathbf{x}^i) & \text{for } i \in I_{int}, \\ \gamma \sum_{j=1}^M \hat{u}_j(\Delta\varphi_j(\mathbf{x}^i)) = k(\sum_{j=1}^M \hat{y}_j\varphi_j(\mathbf{x}^i) - z(\mathbf{x}^i)) & \text{for } i \in I_{int}, \\ \sum_{j=1}^M \hat{y}_j\varphi_j(\mathbf{x}^i) = 0, & \text{for } i \in I_{bd}, \\ \sum_{j=1}^M \hat{u}_j\varphi_j(\mathbf{x}^i) = 0, & \text{for } i \in I_{bd}. \end{array} \right. \tag{4.2}$$

We use the notations

$$\begin{aligned} \mathbf{F}(\mathbf{x}_{int}) &= [f_j(\mathbf{x}^i)]_{i \in I_{int}, j \in I}, \\ \mathbf{F}(\mathbf{x}_{bd}) &= [f_j(\mathbf{x}^i)]_{i \in I_{bd}, j \in I} \end{aligned}$$

for any $F = (f_1, f_2, \dots, f_m) : \mathbb{R}^n \rightarrow \mathbb{R}^m$, and the bold zero symbol for the zero block matrix with an appropriate size. So, Eqs. (4.2) can be rewritten as a linear vector-matrix product form as

$$\begin{bmatrix} \Delta\Phi(\mathbf{x}_{int}) & k\Phi(\mathbf{x}_{int}) \\ k\Phi(\mathbf{x}_{int}) & -\gamma\Delta\Phi(\mathbf{x}_{int}) \\ \Phi(\mathbf{x}_{bd}) & \mathbf{0} \\ \mathbf{0} & \Phi(\mathbf{x}_{bd}) \end{bmatrix} \begin{bmatrix} \hat{\mathbf{y}} \\ \hat{\mathbf{u}} \end{bmatrix} = \begin{bmatrix} \mathbf{0} \\ k\mathbf{z}(\mathbf{x}_{int}) \\ \mathbf{0} \\ \mathbf{0} \end{bmatrix}, \tag{4.3}$$

where $\hat{\mathbf{y}} = [\hat{y}_i]_{i \in I}^T$ and $\hat{\mathbf{u}} = [\hat{u}_i]_{i \in I}^T$ contain unknown parameters.

Thus, in order to obtain the OCP (2.4) solutions, we just solve the linear system given by Eq. (4.3) to obtain the fuzzy magnitude of \hat{y}_j 's and \hat{u}_j 's. Then using the defuzzifier (3.2) can give the state and control functions as Eq. (3.4) expansions.



4.2. OCP With the Box Constraint Control. In this case, the optimality system is as Eq. (2.11) that contains PDEs associated with a VI. So, we should combine the strategy of solving a VI with the presented method in the previous section. One can reformulate a VI to another algebraic constraint. In particular, reformulating of VI (2.11c) into a linear complementarity problem (LCP) is the most commonly used approach. This approach suggests that Eq. (2.11c) can be replaced by two following LCPs [14]:

$$0 \leq u - g, \lambda_1 \geq 0, \lambda_1 \cdot (u - g) = 0, \tag{4.4a}$$

$$0 \leq h - u, \lambda_2 \geq 0, \lambda_2 \cdot (h - u) = 0, \tag{4.4b}$$

where λ_1 and λ_2 , as Lagrangian functions in $H_0^1(\Omega)$, can be defined by

$$kv + \gamma u + \lambda_2 - \lambda_1 = 0. \tag{4.5}$$

Indeed, Eqs. (4.4) and (4.5) are the strong form of VI (2.11c). It can be easily observed that any solution of VI (2.11) solves Eqs. (4.4) and (4.5), and vice versa. By removing v from Eqs. (2.11b) and (4.5), the first-order optimality system reduces as

$$\Delta y + ku = 0, \tag{4.6a}$$

$$ky - \gamma \Delta u - \Delta(\lambda_2 - \lambda_1) = kz, \tag{4.6b}$$

$$0 \leq u - g, \lambda_1 \geq 0, \lambda_1 \cdot (u - g) = 0, \tag{4.6c}$$

$$0 \leq h - u, \lambda_2 \geq 0, \lambda_2 \cdot (h - u) = 0, \tag{4.6d}$$

$$y = 0 \quad \text{and} \quad u = 0 \quad \text{on} \quad \partial\Omega. \tag{4.6e}$$

By the fuzzy representation of the Lagrangian functions λ_1 and λ_2 and also the state and control functions in Eq. (3.4), we can collocate Eqs. (4.6) in the computational points Σ . Complementarity conditions and differential equations are collocated only at the interior points. Therefore, the discretizations of Eqs. (4.6c) and (4.6d) are in the form

$$\begin{cases} 0 \leq \sum_{j=1}^M \hat{\lambda}_{1,j} \varphi_j(\mathbf{x}^i) \perp \sum_{j=1}^M (\hat{u}_j - \hat{g}_j) \varphi_j(\mathbf{x}^i) \geq 0, & i \in I_{int}, \\ 0 \leq \sum_{j=1}^M \hat{\lambda}_{2,j} \varphi_j(\mathbf{x}^i) \perp \sum_{j=1}^M (\hat{h}_j - \hat{u}_j) \varphi_j(\mathbf{x}^i) \geq 0, & i \in I_{int}. \end{cases} \tag{4.7}$$

The symbol \perp stands for the complementarity constraint. Positive values of the FBFs in the whole set \mathbb{R} conclude the following conditions and ensure that Eqs. (4.7) are met each other:

$$\mathbf{0} \leq \begin{bmatrix} \hat{\lambda}_1 \\ \hat{\lambda}_2 \end{bmatrix} \perp \begin{bmatrix} \hat{\mathbf{u}} - \hat{\mathbf{g}} \\ \hat{\mathbf{h}} - \hat{\mathbf{u}} \end{bmatrix} \geq \mathbf{0}. \tag{4.8}$$

Therefore, the optimality conditions are a mixed complementarity problem as

$$\begin{bmatrix} \Delta\Phi(\mathbf{x}_{int}) & k\Phi(\mathbf{x}_{int}) & \mathbf{0} & \mathbf{0} \\ k\Phi(\mathbf{x}_{int}) & -\gamma\Delta\Phi(\mathbf{x}_{int}) & \Delta\Phi(\mathbf{x}_{int}) & -\Delta\Phi(\mathbf{x}_{int}) \\ \Phi(\mathbf{x}_{bd}) & \mathbf{0} & \mathbf{0} & \mathbf{0} \\ \mathbf{0} & \Phi(\mathbf{x}_{bd}) & \mathbf{0} & \mathbf{0} \end{bmatrix} \begin{bmatrix} \hat{\mathbf{y}} \\ \hat{\mathbf{u}} \\ \hat{\lambda}_1 \\ \hat{\lambda}_2 \end{bmatrix} = \begin{bmatrix} \mathbf{0} \\ kz(\mathbf{x}_{int}) \\ \mathbf{0} \\ \mathbf{0} \end{bmatrix}, \tag{4.9}$$

$$\mathbf{0} \leq \begin{bmatrix} \hat{\lambda}_1 \\ \hat{\lambda}_2 \end{bmatrix} \perp \begin{bmatrix} \hat{\mathbf{u}} - \hat{\mathbf{g}} \\ \hat{\mathbf{h}} - \hat{\mathbf{u}} \end{bmatrix} \geq \mathbf{0}.$$

Here, the bold letters in the RHS vector and the coefficients matrix are defined as mentioned before and the fuzzy parameters put into the vectors $\hat{\mathbf{u}} = [\hat{u}_i]_{i \in I}$, $\hat{\mathbf{y}} = [\hat{y}_i]_{i \in I}$, $\hat{\lambda}_1 = [\hat{\lambda}_{1,i}]_{i \in I}$, and $\hat{\lambda}_2 = [\hat{\lambda}_{2,i}]_{i \in I}$ as the unknown vectors.

One of the common approaches to deal with the complementarity problem (4.9) is to convert it to a classical system of equations using a *C-function* [15]. A function $\mathbf{F} : \mathbb{R}^n \times \mathbb{R}^n \rightarrow \mathbb{R}^n$ is called C-function if for any pair $(\mathbf{a}, \mathbf{b}) \in \mathbb{R}^n \times \mathbb{R}^n$, we have

$$0 \leq \mathbf{b} \perp \mathbf{a} \geq 0 \quad \Leftrightarrow \quad \mathbf{F}(\mathbf{a}, \mathbf{b}) = 0. \tag{4.10}$$



It is noteworthy that in a general manner, the complementarity conditions can be replaced by a smooth C-function. However, the smooth reformulation always leads to a system of equations with singular Jacobian and hence the development of a proper numerical method fails in this case [8]. One of the famous non-smooth C-functions is the Fischer-Burmeister function [16] given by the rule

$$\varphi_{FB}(\mathbf{a}, \mathbf{b}) := \mathbf{b} + \mathbf{a} - \sqrt{\mathbf{b}^2 + \mathbf{a}^2}. \tag{4.11}$$

Hence using the FB C-function, the LCP (4.8) can be substituted by the nonlinear system

$$\begin{pmatrix} \varphi_{FB}(\hat{\lambda}_1, \hat{\mathbf{u}} - \hat{\mathbf{g}}) \\ \varphi_{FB}(\hat{\lambda}_2, \hat{\mathbf{h}} - \hat{\mathbf{u}}) \end{pmatrix} = \mathbf{0} \tag{4.12}$$

and it can be substituted for the complementarity conditions in Eqs. (4.9). Therefore, the optimality conditions yield the following nonlinear system of equations:

$$\mathbf{F}(\mathbf{v}) := \begin{pmatrix} \Delta\Phi(\mathbf{x}_{int})\hat{\mathbf{y}} + k\Phi(\mathbf{x}_{int})\hat{\mathbf{u}} \\ k\Phi(\mathbf{x}_{int})\hat{\mathbf{y}} - \gamma\Delta\Phi(\mathbf{x}_{int})\hat{\mathbf{u}} + \Delta\Phi(\mathbf{x}_{int})(\hat{\lambda}_1 - \hat{\lambda}_2) \\ \Phi(\mathbf{x}_{bd})\hat{\mathbf{y}} \\ \Phi(\mathbf{x}_{bd})\hat{\mathbf{u}} \\ \varphi_{FB}(\hat{\lambda}_1, \hat{\mathbf{u}} - \hat{\mathbf{g}}) \\ \varphi_{FB}(\hat{\lambda}_2, \hat{\mathbf{h}} - \hat{\mathbf{u}}) \end{pmatrix} = \mathbf{0}, \tag{4.13}$$

where $\mathbf{v} = (\hat{\mathbf{y}}, \hat{\mathbf{u}}, \hat{\lambda}_1, \hat{\lambda}_2)$. Eq. (4.13) is not differentiable system and usual Newton method fails to solve it. In fact, Eq. (4.13) is a semi-smooth system of equations. One can use *semi-smooth Newton* (SSN) method to solve it.

The SSN method is an iterative method in which the Clarke generalized Jacobian, denoted here by $\partial\mathbf{F}$, is used instead of the classic definition of Jacobian [16]. In order to solve Eqs. (4.13), in the k -th iteration of the SSN method, the new value of \mathbf{x} is updated by $\mathbf{v}^{k+1} = \mathbf{v}^k + h^k$, where the correct value of h^k can be computed by solving

$$-[J_F(\mathbf{v}^k)]h^k = \mathbf{F}(\mathbf{v}^k), \tag{4.14}$$

where $J_F \in \partial\mathbf{F}$. Algorithm 1 summarizes the general scheme of the SSN method to solve $\mathbf{F}(\mathbf{v}) = \mathbf{0}$.

Algorithm 1 General scheme of the SSN method

- Initialize** Choose $\mathbf{v}^0 \in \mathbb{R}^n$.
 - Choose $\epsilon > 0$ as the upper bound of the error.
 - Set $k \leftarrow 0$.
 - Step 1** If $\|\mathbf{F}(\mathbf{v}^k)\| < \epsilon$, then stop.
 - Step 2** Select an element $J_F(\mathbf{v}^k) \in \partial\mathbf{F}(\mathbf{v}^k)$.
 - Find a direction $h^k \in \mathbb{R}^n$ such that $\mathbf{F}(\mathbf{v}^k) + J_F(\mathbf{v}^k)h^k = \mathbf{0}$.
 - Step 3** Set $\mathbf{v}^{k+1} = \mathbf{v}^k + h^k$ and $k \leftarrow k + 1$. Return back to Step 1.
-

Thus, in order to find the OCP (2.4) solutions, we solve the linear system (4.13) to obtain the fuzzy magnitude of \hat{y}_j 's and \hat{u}_j 's, by the presented SSN method. Then the defuzzifier (3.2) can be made the control and state functions as expansions given by Eq. (3.4).

Remark 4.1. It is worth noting that the bilateral constraint (2.4d) can be replaced by unilateral constraint $u(x) \leq h(x)$ (or $g(x) \leq u(x)$) in some cases. It means that we can set $u_a = -\infty$ (or $u_b = \infty$). In this situation, the VI (2.11c) is equivalent to complementarity conditions obtained by substituting $\lambda_1 = 0$ (or $\lambda_2 = 0$) into Eq. (4.5) and eliminating extra condition (4.4a) (or (4.4b)).



4.3. Convergence analysis. In this section, we will discuss convergence of the presented semi-smooth Newton method which has been described in Algorithm 1. In general speaking, it is well known that semi-smooth Newton family methods have superlinear convergence. For example, in [6, 9, 26, 28] and some other papers, under different regularity conditions, superlinear convergence of SSN method for a semi-smooth system have been proved. To enter the discussion, it is necessary to provide a clear definition of the semi-smooth function.

Definition 4.2. [26] A function $f : \mathbb{R}^n \rightarrow \mathbb{R}^m$ is said to be semi-smooth at x if it is locally Lipschitz and, for all h , the following limit exists and is finite:

$$\lim_{\substack{M \in \partial f(x+t\bar{h}) \\ \bar{h} \rightarrow h}} M\bar{h}.$$

Also, for $0 < p \leq 1$, the function f is p -order semi-smooth at x , if it is locally Lipschitz and directionally differentiable at x , and if

$$\max_{M \in \partial f(x+h)} \|Mh - f'(x, h)\|_2 = O(\|h\|_2^{1+p}), \quad h \rightarrow 0. \quad (4.15)$$

It can be proven that Fischer-Burmeister C-function is a 1-order semi-smooth function [9]. The following lemma about p -order semismooth function will be useful in the convergence theorem.

Lemma 4.3. [28] *Let f be p -order semismooth at x . Then we have*

$$\max_{M \in \partial f(x+h)} \|f(x+h) - f(x) - Mh\|_2 = O(\|h\|_2^{1+p}), \quad h \rightarrow 0, \quad (4.16)$$

$$\|f(x+h) - f(x) - f'(x, h)\|_2 = O(\|h\|_2^{1+p}), \quad h \rightarrow 0. \quad (4.17)$$

Now, we present the next convergence theorem for the SSN method described in Algorithm 1.

Theorem 4.4. *Suppose that \mathbf{v}^* is a solution of (4.13). If the interpolation matrix $\mathbf{A} = [\varphi_i(x_j)]$ is nonsingular, then the iteration method (4.14) is well-defined and it has quadratic convergence to \mathbf{v}^* in a neighborhood of \mathbf{v}^* .*

Proof. By the definition of the Clarke generalized Jacobian, we can define

$$J_F := \begin{bmatrix} \Delta\Phi(\mathbf{x}_{int}) & k\Phi(\mathbf{x}_{int}) & \mathbf{0} & \mathbf{0} \\ k\Phi(\mathbf{x}_{int}) & -\gamma\Delta\Phi(\mathbf{x}_{int}) & \Delta\Phi(\mathbf{x}_{int}) & -\Delta\Phi(\mathbf{x}_{int}) \\ \Phi(\mathbf{x}_{bd}) & \mathbf{0} & \mathbf{0} & \mathbf{0} \\ \mathbf{0} & \Phi(\mathbf{x}_{bd}) & \mathbf{0} & \mathbf{0} \\ \mathbf{0} & \partial_1(\hat{\lambda}_1^k, \hat{\mathbf{u}} - \hat{\mathbf{g}}) & \partial_2(\hat{\lambda}_1^k, \hat{\mathbf{u}} - \hat{\mathbf{g}}) & \mathbf{0} \\ \mathbf{0} & \partial_1(\hat{\lambda}_2^k, \hat{\mathbf{h}} - \hat{\mathbf{u}}^k) & \mathbf{0} & -\partial_2(\hat{\lambda}_2^k, \hat{\mathbf{h}} - \hat{\mathbf{u}}^k) \end{bmatrix}, \quad (4.18)$$

where $\partial_i(\mathbf{a}, \mathbf{b}) := \text{diag}(I_i(\mathbf{a}, \mathbf{b}))$ for $i = 1, 2$, and

$$I_1(\mathbf{a}, \mathbf{b}) := \begin{cases} (1-s) & a_i = b_i = 0, \\ (1 - b_i(a_i^2 + b_i^2)^{-1/2}) & \text{otherwise,} \end{cases} \quad (4.19)$$

$$I_2(\mathbf{a}, \mathbf{b}) := \begin{cases} (1-q) & a_i = b_i = 0, \\ (1 - a_i(a_i^2 + b_i^2)^{-1/2}) & \text{otherwise,} \end{cases} \quad (4.20)$$

where s and q are real positive numbers such that $s^2 + q^2 = 1$. By block partitioning of the generalized Jacobian J_F , it can be seen that

$$\det(J_F) = k^{2N} (\det(\mathbf{A}))^2 \det(\partial_2(\hat{\lambda}_1^k, \hat{\mathbf{u}} - \hat{\mathbf{g}})) \det(\partial_2(\hat{\lambda}_2^k, \hat{\mathbf{h}} - \hat{\mathbf{u}})).$$

Therefore, the nonsingularity of $J_F \in \partial \mathbf{F}(\mathbf{v}^*)$ is guaranteed by assumption of nonsingularity of the interpolation matrix \mathbf{A} . Then there is a neighborhood $\mathcal{N}(\mathbf{v}^*)$ and a constant C such that for any $\mathbf{w} \in \mathcal{N}(\mathbf{v}^*)$ and any $M \in \partial \mathbf{F}(\mathbf{w})$, M is nonsingular and $\|M^{-1}\| \leq C$ (for details see Proposition 3.1. of [26]). On the other hand, 1-order semi-smoothness of



FB C-function leads to 1-order semi-smoothness of \mathbf{F} , straightforwardly. Now, starting from $\mathbf{v}^0 \in \mathcal{N}(\mathbf{v}^*)$, and using (4.15) and (4.17), we have

$$\begin{aligned} \|\mathbf{v}^{k+1} - \mathbf{v}^*\| &= \|\mathbf{v}^k - [J_F(\mathbf{v}^k)]^{-1}\mathbf{F}(\mathbf{v}^k) - \mathbf{v}^*\| \\ &\leq \|[J_F(\mathbf{v}^k)]^{-1} [\mathbf{F}(\mathbf{v}^k) - \mathbf{F}(\mathbf{v}^*) - \mathbf{F}'(\mathbf{v}^*; \mathbf{v}^k - \mathbf{v}^*)]\| \\ &\quad + \|[J_F(\mathbf{v}^k)]^{-1} [J_F(\mathbf{v}^k)(\mathbf{v}^k - \mathbf{v}^*) - \mathbf{F}'(\mathbf{v}^*; \mathbf{v}^k - \mathbf{v}^*)]\| \\ &= O(\|\mathbf{v}^k - \mathbf{v}^*\|^2). \end{aligned}$$

□

5. NUMERICAL TESTS

Here, we perform some numerical experiments to show the efficiency and the accuracy of the presented method. Our numerical examples are selected from the benchmark problems and cover all described modes of the given problem, including non-constrained, unilateral and bilateral constrained optimal control.

The numerical experiments are carried out by utilizing MATLAB R2017b on a Core i5 (3.6 GHz) PC with 8GB of RAM. We set $a_i^j = 1$ and $\sigma_i^j = 30$ for all i and j in the definition of the FBFs. Moreover, the mean values of the Gaussian functions are set as same as the computational points Σ , i.e., $\mathbf{m}^j = (m_1^j, m_2^j) = (x_1^j, x_2^j) \in \Sigma$ for all $j \in I$. We consider uniform partitions with K number of points in each direction. Hence the total number of fuzzy rule bases is $M = K^2$. Also, in order to define the Jacobian matrix $J_F(\mathbf{v}^k)$ to use in the fuzzy system-based semi-smooth Newton method, the parameters in Eqs. (4.19)-(4.20) are set as $p = 0.6$ and $q = 0.8$. Moreover, our reports for objective functional values need to integration in Ω . It is carried out by using of Legendre-Gauss-Lobatto quadrature with the number of 30 points in each axis.

Example 5.1. As the first numerical example, we consider the OCP (2.4), where $\Omega = [0, 1]^2$ and $\mathcal{U} = L^2(\Omega)$. Also, in the whole domain,

$$z(\mathbf{x}) = \sin(\pi x_1) \sin(\pi x_2).$$

If we set $k = 1$, this example has an exact optimal solution for any $\gamma > 0$ in the form [10]

$$y_{opt}(\mathbf{x}) = C(\gamma) \sin(\pi x_1) \sin(\pi x_2), \tag{5.1}$$

$$u_{opt}(\mathbf{x}) = 2\pi^2 C(\gamma) \sin(\pi x_1) \sin(\pi x_2), \tag{5.2}$$

where $C(\gamma) = \frac{1}{1+4\gamma\pi^4}$ is a constant depending only on γ .

First, we apply the presented method for this example with different values of γ . Table 1 contains absolute errors in L^2 -norm using different values of M and γ . Here, y^*, u^* and J^* are the state function, the control function and the objective functional value obtained from the presented method, respectively. They are compared with exact values for each case in Table 1. This table shows the convergence of the method by increasing the discretization parameter M for any γ . The third row of each case shows the approximation of the absolute error of the objective function. Also, Figure 2 shows the absolute error of the approximated state and control functions for $\gamma = 0.1$ obtained by applying the presented method with $K = 35$.

To compare the presented method with other schemes, we solve this example for different values of γ using our FBF method and also the radial base function collocation method (RBFC) presented in [23] with the same number of basis functions $K = 35$. We also solve this example with the finite elements (FE) method having 900 elements in the domain. Numerical results are reported in Table 2. In the same conditions, higher capability and efficiency of the FBF method rather than the RBFC and the FE methods are clearly shown.

Moreover, the convergence rate of these three methods are compared in Figure 3 for cases $\gamma = 0.1$ and $\gamma = 10^{-6}$. This figure behaves decreasingly on the absolute error of the objective function obtained values of the methods in the same discretization parameter N . In the presented FBF and the RBFC methods, the discretization parameter is the number of the basis functions, i.e., $N = K^2$, and in the FE method, it is the number of elements in the domain Ω . These diagrams show that the presented method can achieve the accuracy of the machine epsilon range (about 10^{-16}) whenever the absolute errors of the RBFC and the FE methods are between 10^{-5} and 10^{-8} .



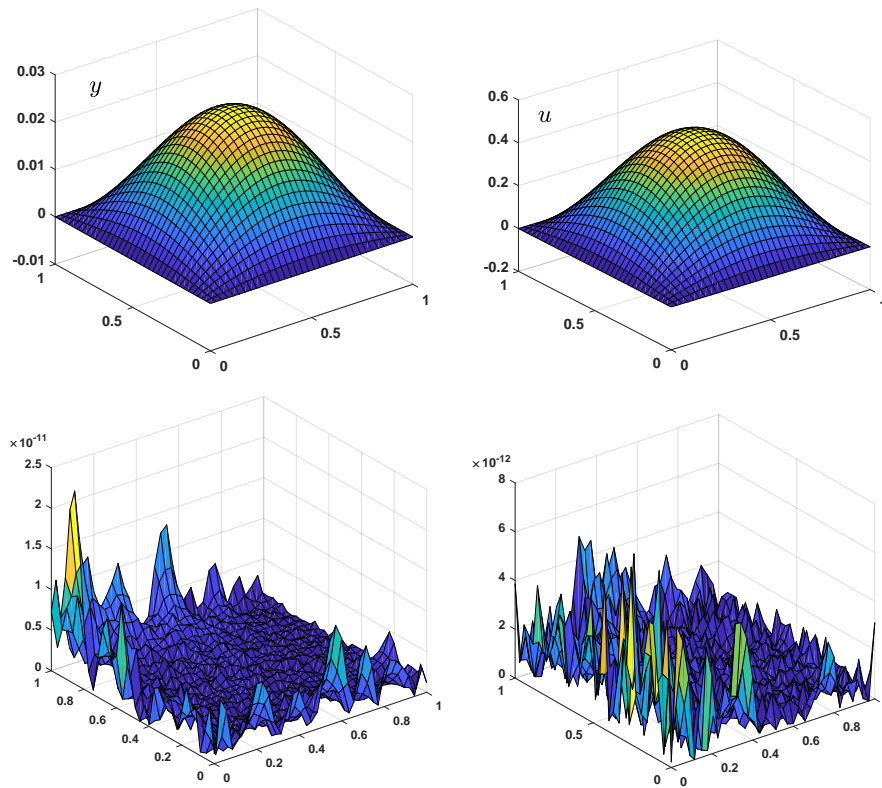


FIGURE 2. The optimal control (above right panel) and the state (above left panel) functions for Example 5.1 (in case $\gamma = 0.1$) obtained by the presented method with $K = 35$ and their absolute errors (below panels).

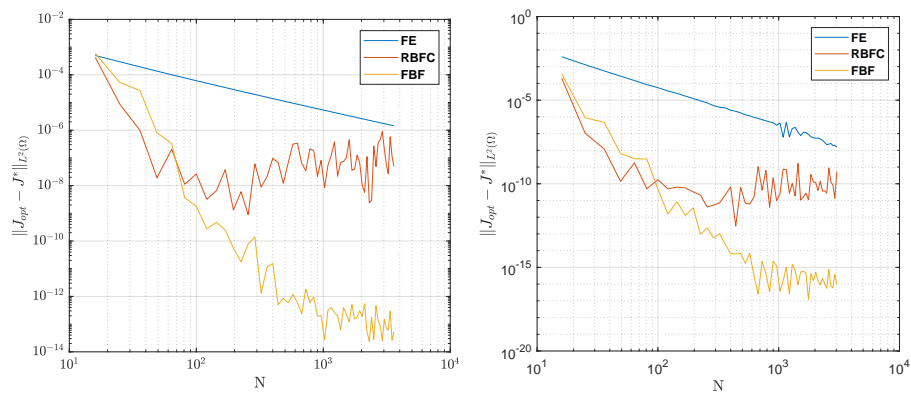


FIGURE 3. The comparison of the convergence rate of different methods for Example 5.1 with $\gamma = 0.1$ (left panel) and $\gamma = 10^{-6}$ (right panel).



TABLE 1. Absolute errors of the state and control functions for Example 5.1 for various values of N and γ .

γ		N			
		25	100	225	900
0.1	$\ y^* - y_{opt}\ _{L^2(\Omega)}$	8.0735e-04	3.0775e-07	9.0501e-08	3.9350e-11
	$\ u^* - u_{opt}\ _{L^2(\Omega)}$	7.5212e-03	2.2648e-06	4.5065e-08	3.5093e-11
	$\ J^* - J_{opt}\ _{L^2(\Omega)}$	5.2834e-05	9.3708e-09	5.5978e-11	6.7174e-13
0.001	$\ y^* - y_{opt}\ _{L^2(\Omega)}$	6.2371e-03	1.9874e-06	6.4469e-07	1.1321e-09
	$\ u^* - u_{opt}\ _{L^2(\Omega)}$	1.1825e-01	2.7879e-05	6.2673e-06	5.2879e-09
	$\ J^* - J_{opt}\ _{L^2(\Omega)}$	4.1143e-04	4.2697e-08	1.1921e-11	4.2437e-13
10^{-5}	$\ y^* - y_{opt}\ _{L^2(\Omega)}$	1.9406e-04	3.0502e-07	1.9330e-07	2.7059e-10
	$\ u^* - u_{opt}\ _{L^2(\Omega)}$	3.1361e-01	1.7866e-04	1.7254e-05	2.2382e-08
	$\ J^* - J_{opt}\ _{L^2(\Omega)}$	6.0433e-06	1.8426e-08	3.8701e-12	1.9415e-14

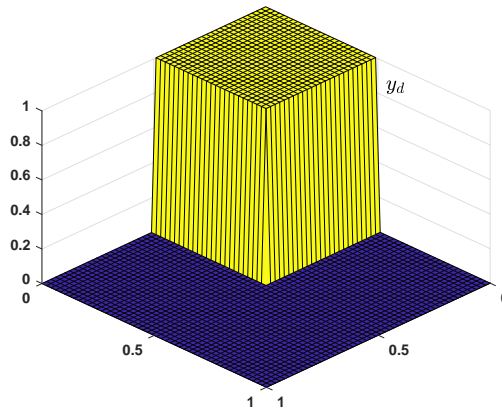


FIGURE 4. Desired state function in Examples 5.2 and 5.3.

Example 5.2. In this example and also in the next one, we focus on a problem from [23]. Consider the OCP (2.4) on $\Omega = [0, 1]^2$ with $\mathcal{U} = L^2(\Omega)$ and $k = 1$, and suppose that

$$z(\mathbf{x}) = \begin{cases} 1 & \mathbf{x} \in [0, \frac{1}{2}]^2, \\ 0 & \text{otherwise} \end{cases} \tag{5.3}$$

is the desired state function shown in Figure 4. Moreover, for $\gamma = 10^{-3}$ and $\gamma = 10^{-5}$, the state and control functions obtained by the developed method with $K = 50$ is given in Figure 5. Some features of the OCP (2.4) solutions are obvious on the figures. As we expected, by reducing the γ coefficient, the state function is getting closer to the desired state function because the smaller values of γ allow us to spend larger values of control function.

Table 3 reports the objective functional values for various values of K and γ . Also, process times for the CPU to solve the problem are reported in milliseconds.

Example 5.3. Here, we study the previous example with different boundary conditions such as

$$y(\mathbf{x}) = f(\mathbf{x}) \quad \mathbf{x} \in \partial\Omega.$$



TABLE 2. The comparison of the fuzzy-based method, the RBFC method presented in [23] and the FE method for Example 5.1 with different values of γ .

γ	Method	$\ y^* - y_{opt}\ _{L^2(\Omega)}$	$\ u^* - u_{opt}\ _{L^2(\Omega)}$	$\ J^* - J_{opt}\ _{L^2(\Omega)}$
1	FBF	5.7745e-11	1.2922e-11	2.3490e-13
	RBFC	1.2550e-04	2.2755e-05	3.7828e-07
	FE	7.2494e-05	7.1330e-04	6.2355e-07
0.1	FBF	3.0737e-10	1.8089e-10	6.7174e-13
	RBFC	9.6477e-05	4.6274e-05	4.0211e-07
	FE	6.9262e-04	6.6570e-03	5.9573e-06
0.01	FBF	5.2992e-11	2.4507e-10	6.1048e-14
	RBFC	1.1535e-05	3.4188e-05	6.6237e-08
	FE	1.0229e-03	3.3811e-02	3.9651e-05
10^{-3}	FBF	7.0513e-10	3.5460e-09	4.2437e-13
	RBFC	2.6632e-04	3.6474e-03	2.6331e-07
	FE	1.0955e-04	8.8541e-02	4.8924e-05
10^{-4}	FBF	2.1802e-09	5.6427e-08	2.7117e-13
	RBFC	3.4446e-05	4.0008e-04	3.6323e-09
	FE	1.2550e-04	2.4914e-01	8.2962e-06
10^{-5}	FBF	1.3082e-09	9.2083e-08	1.9415e-14
	RBFC	6.5490e-05	3.0303e-03	8.3471e-10
	FE	1.2550e-04	2.7656e-01	4.0436e-07
10^{-6}	FBF	3.1239e-10	6.5182e-08	3.0759e-16
	RBFC	3.5320e-04	5.6320e-02	8.6304e-11
	FE	1.1032e-05	2.7948e-01	4.4684e-07

TABLE 3. The objective functional values and the elapsed time for Example 5.2 with various values of K and γ .

K	$\gamma = 0.1$		$\gamma = 0.001$	
	$J^* = J(y^*, u^*)$	CPU (ms)	$J^* = J(y^*, u^*)$	CPU (ms)
10	0.1319588395	0.3	0.1001036988	0.1
15	0.1324469973	0.2	0.1089529186	0.1
20	0.1321160946	0.4	0.0966450066	0.3
25	0.1320697877	1.1	0.0988825970	0.9
30	0.1320658118	2.5	0.0988013440	2.4
40	0.1320591780	7.9	0.0986194553	7.8
50	0.1320581494	17.4	0.0985930005	17.3
55	0.1320533055	27.7	0.0985317105	28.0
60	0.1320536431	43.7	0.0985389244	43.1



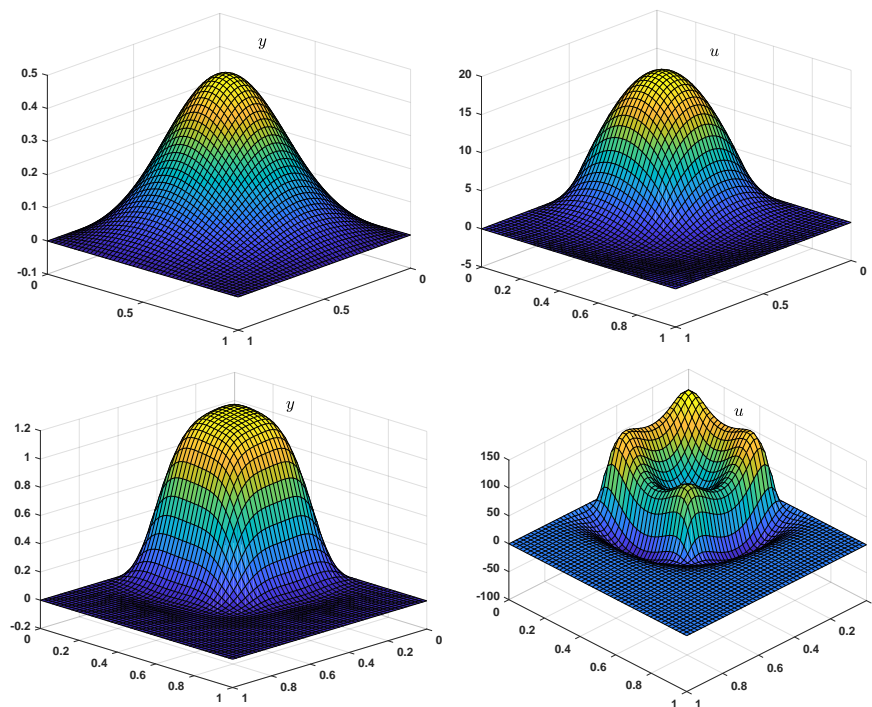


FIGURE 5. The optimal control (right panels) and the state (left panels) functions for Example 5.2 with $\gamma = 10^{-3}$ (above panels) and $\gamma = 10^{-5}$ (below panels) obtained by the presented method with $K = 50$.

In this example, we consider

$$f(\mathbf{x}) = \begin{cases} 1 & \mathbf{x} \in [0, \frac{1}{2}]^2, \\ 0 & \text{otherwise.} \end{cases} \tag{5.4}$$

It can be easily seen that the FBF method is successful to find the optimal control and the state functions in this case, too. The effect of changing the boundary condition is obvious in Figure 6, where the obtained state and control functions from applying the presented method are shown.

Example 5.4. This example devoted to the OCP (2.4) with a unilateral constrained control. Suppose that $\Omega = [0, 1]^2$, $k = 1$ and $\gamma = 0.001$. Then the desired state function is

$$z = \begin{cases} 200x_1x_2(x_1 - 0.5)^2(1 - x_2) & 0 < x_1 \leq 0.5, \\ 200x_2(1 - x_1)(x_1 - 0.5)^2(x_2 - 1) & 0.5 < x_1 \leq 1. \end{cases}$$

The upper restriction of the admissible control is $h(x) = 1$.

The obtained results by utilizing the fuzzy-based SSN algorithm for $K = 35$ are seen in Figure 7. The related Lagrangian function for the final solutions is shown, too. The effect of the control restriction can be evidently seen, where the control touches the upper bound in an elliptic shape subdomain. The small positive values of the Lagrangian function is presented in Figure 7. Hence the complementarity property between the Lagrangian and the control functions is strictly satisfied.

Moreover, this example is solved with various values of γ , to show the efficiency of the fuzzy-based SSN method even for small values of γ . Obtained objective function values for different values K and γ are reported in Table 4. The convergence is emphasized by bold numbers in the reported values. So, it exhibits that the fuzzy-based SSN strategy



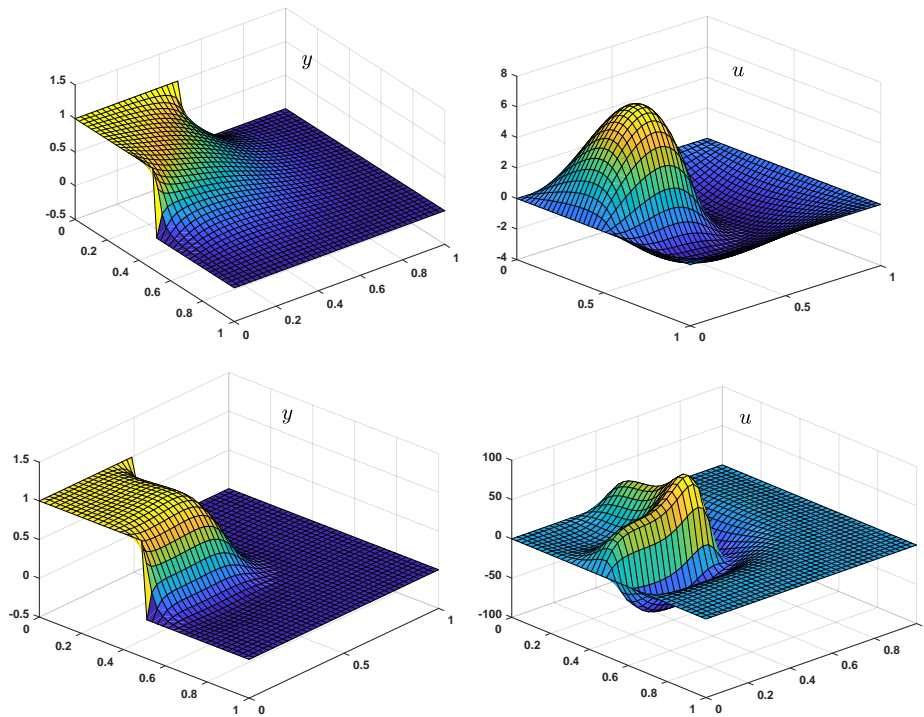


FIGURE 6. The optimal control function (right panels) and the state function (left panels) for Example 5.3 with $\gamma = 10^{-3}$ (above panels) and $\gamma = 10^{-5}$ (below panels) obtained by the presented method with $K = 40$ and their absolute errors.

works properly even for small values of γ . Table 5 reports the CPU times in seconds and the number of iterations of the developed method to solve the problem with $\gamma = 10^{-6}$.

Also, we compared the results of the new algorithm with two other algorithms, A modified active set method described in [4] and an Uzawa method for the augmented Lagrangian with Gauss-Seidel splitting described in [5]. As what is reported in [4], solving this example with $\gamma = 10^{-6}$ and discretization parameter $K = 50$ by modified active set method yields $J_{mas} = 5.839438e - 02$ as the obtained objective functional value. It can be seen that the difference between the obtained objective functional values of Algorithm 1 and modified active set method is

$$|\bar{J}(y^* - u^*) - J_{mas}| = 5.78e - 6.$$

Moreover, one can use the Uzawa type algorithm described in [5] and set the algorithm parameters to achieve similar results, but it takes more CPU time than active set based algorithms [4]. However, our algorithm is terminated after 15 iterations and the processing time is 152.4 seconds and there is not any significant difference between CPU times of Algorithm 1 and modified active set method.

Moreover, we solved this problem by finite difference base semi-smooth Newton method (FD-SSN) [18] as a classical one, and fuzzy active set algorithm [1] in the similar conditions. Nevertheless, semi-smooth Newton method was iterated until the convergence criterion $\|y_{n-1} - y_n\| \leq 10^{-6}$. Table 6 contains results for case $\gamma = 10^{-6}$ and different M values, to compare our presented method with this method.

Example 5.5. Finally, a bilateral control constrained OCP is considered in the last example. Consider $\Omega = [0, 1]^2$ and $k = 1$ and suppose that control function is restricted as

$$-((x_1 - 0.75)^2 + (x_2 - 0.5)^2 + 0.25) \leq u(x_1, x_2) \leq 0.5.$$



TABLE 4. The objective function approximated values by the presented fuzzy-based SSN method for Example 5.4 with different values of K and γ .

K	γ						
	1	10^{-1}	10^{-2}	10^{-3}	10^{-4}	10^{-5}	10^{-6}
15	0.09909853	0.09825741	0.08460142	0.07552998	0.06095336	0.05546934	0.05450265
20	0.09919127	0.09905570	0.09919345	0.09142667	0.07717371	0.06551619	0.06132462
25	0.09918549	0.09899819	0.09901739	0.08946033	0.07447710	0.06380333	0.06017294
30	0.09917500	0.09889378	0.098622608	0.08646815	0.07091474	0.06158264	0.05879545
35	0.09917141	0.09885813	0.09898517	0.08556311	0.07012952	0.06098898	0.05844652
40	0.09917083	0.09840761	0.09891540	0.08541656	0.0700523	0.06089871	0.05842535
45	0.09917066	0.09885072	0.09890813	0.0853724	0.0700411	0.06086961	0.05840180
50	0.09917065	0.09885072	0.09890461	0.08583443	0.0700481	0.06086642	0.05840016

TABLE 5. The objective function values, the number of the iterations and the CPU time of the fuzzy-based SSN algorithm for Example 5.4 with $\gamma = 10^{-6}$ and various values of K .

K	J^*	Nit.	CPU(s)
15	0.05450265	9	0.25
20	0.06132462	11	0.94
25	0.06017294	12	3.26
30	0.05879545	15	11.2
35	0.05844652	14	24.55
40	0.05842535	14	49.69
45	0.05840180	14	90.65
50	0.05840016	15	152.4

We carry out the developed fuzzy-based SSN algorithm on the current example with $\gamma = 10^{-1}, 10^{-2}, 10^{-3}$.

The resulted controls, states and related Lagrangian functions by applying the developed algorithm with $K = 35$ are demonstrated in Figure 8. Clearly, it can be seen that the magnitude of γ can make a significant impact on the results.

The greater magnitude of γ means that the control is expensive. So, the small magnitude of the control source is spent. It is clear that if $\gamma = 10^{-1}$, then there exists no touch between the control and the restriction functions. On the other hand, whenever γ decrease to smaller values such as 10^{-3} , spending a larger absolute value of the control function becomes permissive. Thus, the optimal control touches the upper or lower restriction functions in the whole domain. In this case, the problem is called "the bang-bang optimal control". Therefore, the results of this example show the capability of the fuzzy-based SSN algorithm to reveal all properties of the solutions in each case.

6. CONCLUSION

In this paper, a numerical approach based on the fuzzy system was presented to solve the OCP governed by the Poisson's equation. The control function can be constrained or not. We used the universal approximation property of



TABLE 6. Comparison of objective function results the presented method, fuzzy active set algorithm [1] and FD-SSN method [18] for Example 5.4, with various values of M and $\gamma = 10^{-6}$.

M	Fuzzy SSN method	FAS method [1]	FD-SSN method [18]
15	0.05450265	0.04449139	0.10067391
20	0.06132462	0.06062205	0.05189480
25	0.06017294	0.06097321	0.04101627
30	0.05879545	0.05941770	0.04912385
35	0.05844652	0.05859709	0.05734163
40	0.05842535	0.05842535	0.05800691
45	0.05840180	0.05840339	0.05839217
50	0.05840016	0.05840057	0.05843155

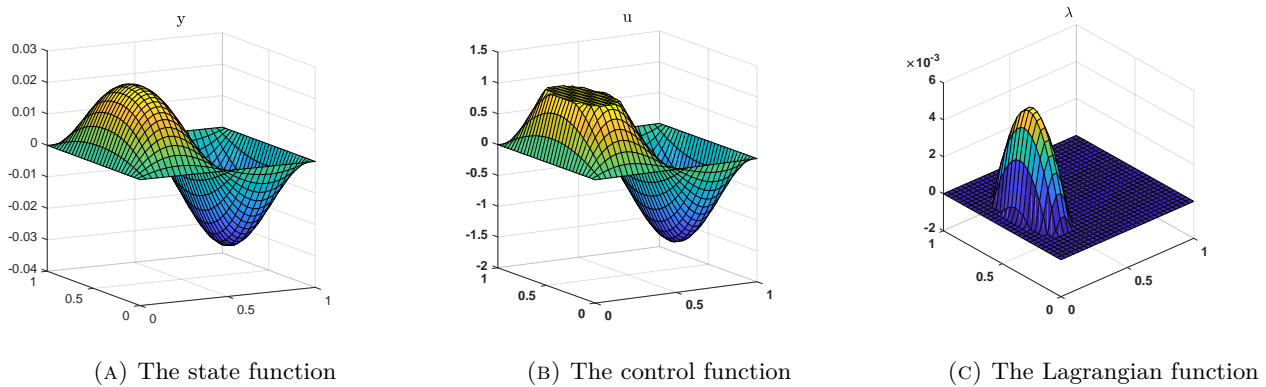


FIGURE 7. The optimal results for Example 5.4.

special FBFs to develop a novel efficient numerical algorithm for the given problem. The selected FBFs were defined by the multi-input-single-output fuzzy product inference and the Gaussian membership functions. More precisely, they were utilized for discretizing of the first-order optimality system such that the original problem is reduced to solve a system of equations ultimately. This system was linear in the non-constrained control case and it could be solved by any linear systems solver. Moreover, in constrained control case, by applying the modified Fischer-Burmeister C-function, the optimality conditions were a non-smooth and non-linear system of equations. To solve this system, a semi-smooth Newton method was combined with the fuzzy-based discretization method. Numerical tests were demonstrated the efficiency and accuracy of the developed algorithm through simulations. It can be observed that the presented algorithm is an appropriate method for the box constrained OCP with non-smooth solutions as well as the smooth ones. CPU run times reported in the examples are extremely low indicating that the fuzzy system provides an efficient tool to solve the given problem.



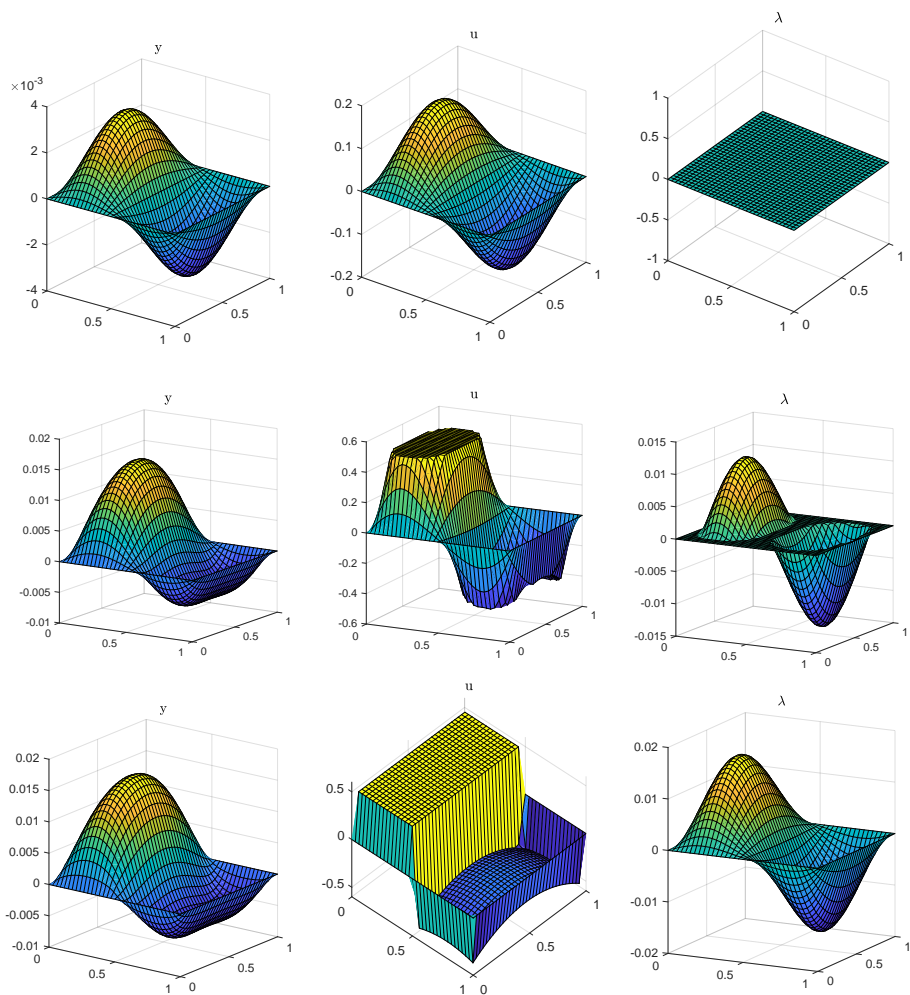


FIGURE 8. The optimal state, the control and the Lagrangian functions for Example 5.5 with various values of γ . In order from the top to the bottom, γ is equal to 10^{-1} , 10^{-2} and 10^{-3} , respectively.

REFERENCES

- [1] M. Azizi, M. Amirfakhrian, and M. A. Fariborzi Araghi, *A fuzzy system based active set algorithm for the numerical solution of the optimal control problem governed by partial differential equation*, Eur. J. Control, *54* (2020), 99–110.
- [2] R. Becker, M. Braack, D. Meidner, R. Rannacher, and B. Vexler, *Adaptive finite element methods for PDE-constrained optimal control problems*, Reactive flows, diffusion and transport, Springer, 2007, 177–205.
- [3] R. Becker, H. Kapp, and R. Rannacher, *Adaptive finite element methods for optimal control of partial differential equations: Basic concept*, SIAM J. Control Optim., *39*(1) (2000), 113–132.
- [4] M. Bergounioux, K. Ito, and K. Kunisch, *Primal-dual strategy for constrained optimal control problems*, SIAM J. Control Optim., *37*(4) (1999), 1176–1194.
- [5] M. Bergounioux and K. Kunisch, *Augmented lagrangian techniques for elliptic state constrained optimal control problems*, SIAM J. Control Optim., *35*(5) (1997), 1524–1543.
- [6] X. Chen, L. Qi and D. Sun, *Global and superlinear convergence of the smoothing newton method and its application to general box constrained variational inequalities*, Math. Comp., *67*(222) (1998), 519–540.
- [7] S. Effati and M. Pakdaman, *Optimal control problem via neural networks*, Neural Comput. & Applic., *23*(7-8) (2013), 2093–2100.
- [8] F. Facchinei and J. -S. Pang, *Finite-dimensional variational inequalities and complementarity problems*, Springer Science & Business Media, 2007.
- [9] A. Fischer, *Solution of monotone complementarity problems with locally lipschitzian functions*, Math. Programming, *76*(3) (1997), Ser. B, 513–532.
- [10] S. Ghasemi and S. Effati, *An artificial neural network for solving distributed optimal control of the Poisson's equation*, Neural Process Lett., *49* (2018), 159–175.
- [11] C. Grossmann, H. -G. Roos, and M. Stynes, *Numerical treatment of partial differential equations*, vol. 154, Springer, 2007.
- [12] M. Gugat and M. Herty, *The smoothed-penalty algorithm for state constrained optimal control problems for partial differential equations*, Optim. Methods Softw., *25*(4-6) (2010), 573–599.
- [13] M. Hintermüller and R. H. W. Hoppe, *Goal-oriented adaptivity in control constrained optimal control of partial differential equations*, SIAM J. Control Optim., *47*(4) (2008), 1721–1743.
- [14] M. Khaksar-e Oshagh and M. Shamsi, *Direct pseudo-spectral method for optimal control of obstacle problem—an optimal control problem governed by elliptic variational inequality*, Math. Methods Appl. Sci., *40*(13) (2017), 4993–5004.
- [15] M. Khaksar-e Oshagh and M. Shamsi, *An adaptive wavelet collocation method for solving optimal control of elliptic variational inequalities of the obstacle type*, Comput. Math. Appl., *75*(2) (2018), 470–485.
- [16] M. Khaksar-e Oshagh, M. Shamsi, and M. Dehghan, *A wavelet-based adaptive mesh refinement method for the obstacle problem*, Engineering with Computers, *34*(3) (2018), 577–589.
- [17] H. M. Kim and J. M. Mendel, *Fuzzy basis functions: Comparisons with other basis functions*, IEEE Trans. Fuzzy Syst., *3*(2) (1995), 158–168.
- [18] A. Kröner, K. Kunisch, and B. Vexler, *Semismooth newton methods for optimal control of the wave equation with control constraints*, SIAM J. Control Optim., *49*(2) (2011), 830–858.
- [19] R. Li, W. Liu, H. Ma, and T. Tang, *Adaptive finite element approximation for distributed elliptic optimal control problems*, SIAM J. Control Optim., *41*(5) (2002), 1321–1349.
- [20] W. Liu and N. Yan, *A posteriori error estimates for distributed convex optimal control problems*, Adv. Comput. Math., *15*(1-4) (2001), 285–309.
- [21] M. A. Mehrpouya and M. Khaksar-e Oshagh, *An efficient numerical solution for time switching optimal control problems*, Comput. Methods Differ. Equ., *9*(1) (2021), 225–243.
- [22] M. Pakdaman and S. Effati, *Approximating the solution of optimal control problems by fuzzy systems*, Neural Process Lett., *43*(3) (2016), 667–686.
- [23] J. W. Pearson, *A radial basis function method for solving PDE-constrained optimization problems*, Numer. Algor., *64*(3) (2013), 481–506.



- [24] J. W. Pearson and A. J. Wathen, *A new approximation of the Schur complement in preconditioners for PDE-constrained optimization*, Numer. Linear Algebra Appl., *19*(5) (2012), 816–829.
- [25] H. Pourbashash and M. Khaksar-e Oshagh, *Local RBF-FD technique for solving the two-dimensional modified anomalous sub-diffusion equation*, Appl. Math. Comput., *339* (2018), 144–152.
- [26] L. Qi and J. Sun, *A nonsmooth version of newton's method*, Math. Programming, *58*(1) (1993), 353–367.
- [27] F. Tröltzsch, *Optimal control of partial differential equations: theory, methods, and applications*, vol. 112, American Mathematical Society, 2010.
- [28] M. Ulbrich, *Semismooth newton methods for operator equations in function spaces*, SIAM J. Optim., *13*(3) (2002), 805–841.
- [29] L. X. Wang and J. M. Mendel, *Back-propagation fuzzy system as nonlinear dynamic system identifiers*, IEEE International Conference on Fuzzy Systems, *8* (1992), 1409–1418.
- [30] L. X. Wang and J. M. Mendel, *Fuzzy basis functions, universal approximation, and orthogonal least-squares learning*, IEEE Transactions on Neural Networks, *3*(5) (1992), 807–814.

